# SYMMETRY-PRESERVING DISCRETIZATIONS IN UNSTRUCTURED STAGGERED MESHES


***N. Valle[1,2], F.X. Trias[1] and R.W.C.P. Verstappen[2]***

[1] ***Heat and Mass Transfer Technological Center, Technical University of Catalonia, ETSEIAT, c/Colom 11, 08222 Terrassa, Spain***
[2] ***Bernoulli Institute, University of Groningen, PO Box 407, 9700AK Groningen, the Netherlands***

**n.valle.marchante@rug.nl**



## Abstract

The adoption of symmetry-preserving discretizations is presented in terms of the collocated, unstructured meshes customary of commercial codes. By adopting an algebraic approach, a discretization of the convective terms that reduces to the well know staggered method of Harlow and Welch is presented. The scheme properties are presented along with benchmark simulations concerning turbulent flows, achieving exact conservation of momentum and kinetic energy.


## 1 Introduction

Since the pioneering work of Harlow and Welch (1965), the use of staggered variables has gained widespread acceptance within the scientific community due to its superior properties for the simulation of incompressible flows. Its use along with symmetry-preserving schemes as in Morinishi et al. (1998), Vasilyev (2000), and Verstappen and Veldman (1997, 2003) sets the standard of high quality, state-of-the-art Direct Numerical Simulation of turbulent flows. However, despite its known advantages, the popularity drops dramatically in commercial, unstructured codes. The main reason behind it is the complex formulation required to move from a structured arrangement to an unstructured one when it comes to construct an overlapping, staggered mesh; particularly when dealing with the construction of the convective term.

While several attempts have been made in the past to bring these ideas into unstructured meshes, there is none, to the best of our knowledge, that recovers the original Harlow and Welch formulation when applied to a structured one. Perot (2000) and Zhang et al. (2002a) discussed its implementation by interpolating the collocated discretization to the faces, while numerical patologies appeared on its way. Later on, Hicken et al. (2005) introduced a new type of shift transformations to address such a problem. However, none of the methods introduced above recovers the original Harlow and Welch formulation when applied to structured meshes.

Trias et al. (2014) presented an alternative approach involving the construction of collocated discretizations that preserve symmetry. Nonetheless, this clashes with the solution of the compact Laplace equation, which solves pressure by enforcing null divergence of the staggered velocity as Trias et al. (2021). While this mismatch can be fixed by interpolation, this may enlarge the kernel dimension of the overall linear system of equations, giving birth to the well-known checker board problem. While numerical remedies can be found, such as the popular Rhie and Chow (1983) method, this introduces a mass conservation error Trias et al. (2021).

A remarkable attempt to bring staggered formulations into unstructured meshes was the adoption of the vorticity formulation. By locating vorticity at the mesh edges it was better suited for an unstructured mesh. Nonetheless, as was shown by Horiuti and Itami (1998), this formulation does not collapse to the skew-symmetric one unless homogeneous Cartesian meshes are used. In addition, as presented by Zhang et al. (2002a), this formulation does indeed preserve kinetic energy and vorticity, while it is unsuitable for the conservation of kinetic energy and linear momentum at the same time, suggesting the use of the divergence form instead.

The geometric intuition behind the adoption of the rotational form was to cleverly circumvent the construction of an explicit staggered mesh, which may turn cumbersome in unstructured meshes. However, the ultimate reason between the mismatch between rotational and discrete forms at the discrete level was the lack of a discrete chain rule Horiuti and Itami (1998). In this work, similarly to the computation of discrete vorticity, we embrace the idea of computing quantities at the collocated edges but enforce the fulfillment of the discrete conservation form. To do so, we use primal and dual meshes, as well as conservative interpolations between different geometric entities. Making use of the aforementioned collocated operators only, we present a new discretization of the convective term which recovers the classical Harlow and Welch formulation when applied to a Cartesian mesh, but that is also suitable for unstructured meshes.

Equipped with such a discretization, we assess the properties of staggered scheme against previous proposals advocating for the interpolation of the collocated discretizations.

## 2 Mathematical formulation

**Collocated**

We consider a classical mesh as a coherent collection geometrical entities in an $n$-dimensional space. When $n = 3$, we talk about the set of points, edges, faces and cells, which define the sets $P$, $L$, $S$, and $V$, respectively. These are sequenced by its corresponding incidence matrices, $E_i$, as can be seen in Figure 2. Incidence matrices represent the boundary elements of every higher dimensional set (i.e.: two points bound an edge, edges bound faces and finally faces bound cells). These incidence matrices are signed, which account for boundaries **orientation**. Each element of the mesh can be given a **metric**, which are arranged as diagonal matrices $M_i$ i.e.: identity ($dx^0$), length ($dx^1$), surface ($dx^2$) and volume ($dx^3$), respectively.

For every geometric entity we may define its corresponding **wedge dual**, which define the sets $\widetilde{P}$, $\widetilde{L}$, $\widetilde{S}$, and $\widetilde{V}$, corresponding to the volume centroids, the face orthogonal lines, the lines orthogonal faces and the point volumes, respectively. Those are equipped with its metric as well and are related to each other by a sequence of $\widetilde{E_i} = E^T_{n-i}$. Analogously, the operators $\widetilde{G}$, $\widetilde{C}$ and $\widetilde{D}$ can be constructed as in Lipnikov et al. (2014), although additional conditions may be imposed on the mesh VanderZee et al. (2010). Although these quantities require a bit more effort to obtain from the mesh, they are readily used most of the time under the hood of most discretization methods.

Physical quantities can be integrated (i.e., discretized) over each of these sets. Depending on its physical nature Tonti (1975, 2014), they naturally fit in one or another. For example: temperature $T$ naturally fits in $P$; and its gradient $dT$ is naturally integrated along $\widetilde{L}$; while the heat flux $f$ belongs to $\widetilde{S}$ owing to its flux nature but also to its link with the temperature gradient as $\underset{\sim}{f} = \lambda dT$; finally, thermal energy $e$ naturally fits in $\widetilde{V}$ as $df = e$ but also because $e = CpT$.

These matrices can be readily obtained from the mesh, and allow to construct discrete classical vector calculus operators:

$$\widetilde{G}\phi_c = \widetilde{M_1}^{-1}\widetilde{E_0}\widetilde{M_0}\phi_c = \frac{1}{\Delta x}\sum_{c\in f} \pm\phi_c \qquad \forall f \quad (1)$$

$$C\phi_c = M_2^{-1}E_1M_1\phi_e = \frac{1}{S_f}\sum_{e\in f} \pm L_e\phi_e \quad \forall f \quad (2)$$

$$D\phi_f = M_3^{-1}E_2M_2\phi_f = \frac{1}{V_c}\sum_{f\in c} \pm S_f\phi_f \quad \forall c \quad (3)$$

where $\pm$ sign accounts for the orientation with respect to the element under consideration. This information is readily included into the incidence matrix, whose rows are in $-1, 0, 1$. Note that $\widetilde{G}$ is the familiar face–located gradient, which corresponds with the dual gradient, while $R$ and $D$ correspond with the curl and divergence, respectively.

The directional derivative, $C(u)\phi$, is used to define the transport of a tensor $\phi$ by a flow $u$. It assigns a flux at every face as $U\Pi_{c\to f}$ where $U = diag(u)$ is the diagonal arrangement of the face-normal flows and $\Pi_{c\to f}$ is the cell-to-face interpolator. This interpolator can be constructed by taking the unsigned matrix $abs(\widetilde{E}_2)$ as $\Pi_{c\to f} = 0.5abs(\widetilde{E}_2)$, which results in the typical center difference scheme. Considering the divergence of the flow, we finally obtain:

$$Cc(u) = DU\Pi_{c\to f} \quad (4)$$

This setup works well for scalar quantities, but what happens if we want to treat **vector** quantities, such as momentum?

Perot (2000) and Zhang et al. (2002b) proposed a double interpolation approach consisting on moving vector components into cell centers, the component-wise application of the collocated convection as in equation (4) and a final interpolation from cell to faces.

$$C_s^0(u) = \Gamma_{c\to s}C_c(u)\Gamma_{s\to c} \quad (5)$$

where $\Gamma_{s\to c}$ is the staggered to collocated interpolator, taking a vector field and $n$-dimensional collocated vector and returning a stagered one, while $\Gamma_{c\to s}$ is the reciprocal operator (i.e., takes a staggered field and return a component-wise collocated one).

However, this approach does not recover the classical Harlow and Welch (1965) approach when applied to a Cartesian mesh. So, how to construct the convective operator in a staggered setup by using the collocated mesh operators?

**Staggered**

In a staggered mesh, we consider the face normals as a new (point) set of vector–valued quantities. Velocity fits naturally in this set. Taking its wedge–dual we obtain the (volume) set of vector-valued quantities. Momentum fits naturally in this one. This staggered control volume can be constructed by taking a face and extruding it along its dual (i.e., orthogonal) line. This results into a prismatic volume which extends at both sides of the face between centroids of the adjacent cells. Its lateral boundaries are defined by the extrusion of the edges bounding the initial face, while a shift of the original face close both ends of the prism. While the explicit construction of the staggered mesh is indeed possible, this involves, most of the times, to dramatically increase the memory demands of the numerical implementation. So we opt instead for defining it in terms of the original, collocated mesh.

Following the same reasoning exposed for the directional derivative in equation (4), we construct the

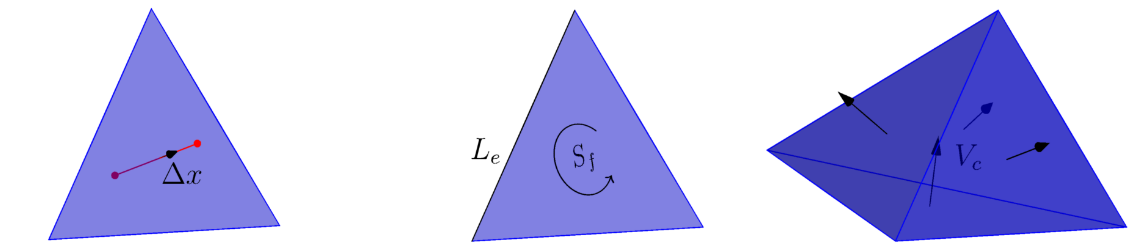


(a) Dual gradient $\widetilde{G}$ (b) Curl $R$ (c) Divergence $D$

Figure 1: Collocated operators defined over and arbitrary unstructured mesh

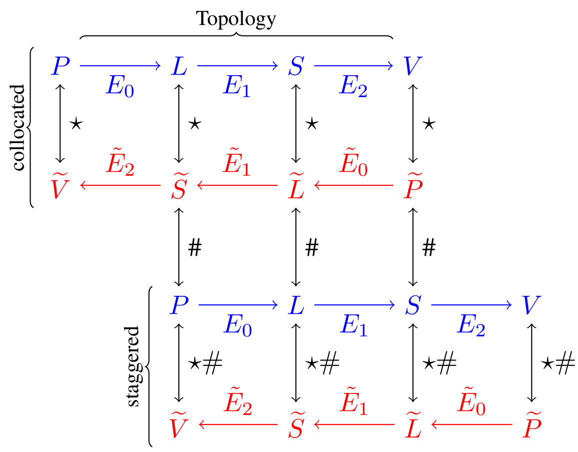


Figure 2: Geometric primal and dual meshes on a collocated arrangement.

vector valued directional derivative. However, the following must be taken under consideration.

First, faces are not, in general, oriented with any preferential direction. This implies that every face contains information from all dimensions of the embedding space, so we approach the problem component-wise, treating each orthogonal direction (i.e., $x$, $y$ and $z$) separately. To do so, we introduce $N = (diag(nx_f)|diag(ny_f)|diag(nz_f))^T \in \mathbb{R}^{3nS \times nS}$, where $ni_f$ is the $i$th component of the face normal, while $nS$ is the number of faces. This maps a face–arranged vector, containing the projection over the normal of the components of the vector field, into a face–arranged vector which contain the $x$, $y$ and $z$ components of the projection. Thus $N\phi$ is the discrete counterpart of $\phi\hat{n}$, which returns the vector $\hat{n}$ scaled by $\phi$. Conversely, the operator $\hat{n} \cdot \vec{v}$ can be represented as $N^T v$, where $v$ is the column arrangement of the vector $\vec{v}$. The adoption of this nomenclature allows to readily extend local vector operations into the whole mesh.

Second, the boundaries of the staggered control volume do not correspond with a unique collocated geometric entity, but rather correspond with the union of $L$ and $V$, i.e., the set of edges and the set of cells. We will treat these two kinds of boundaries separately. In both cases, interpolators $SP_{f\to e}$ and $SP_{f\to\to c}$ are constructed *a la* symmetry preserving, i.e.: by simple arithmetic mean. The values at the boundaries can then be arranged as an $nL + nV$ vector by means of the following block matrix

$$SP_{stg} = \begin{pmatrix} SP_{f\to e} \\ SP_{f\to c} \end{pmatrix} \tag{6}$$

so $(\mathbb{I}_3 \otimes SP_{stg})\, N$ performs the same interpolation on $x$, $y$ and $z$ components.

Third, once we have defined the vector components at the boundaries, we produce the flux of every component multiplying each of them by the corresponding velocity field, $u$, which in turn consists of $n$ dimensions as well. Edge, $\vec{u}_e$, and cell, $\vec{u}_c$, velocities are interpolated from the faces in a volume-weighted fashion, such that the interpolation preserves the volume integral of all quantities. In particular, $\vec{u}_e = 1/2 \left(\widetilde{S_e L_e}\right)^{-1} \sum_{f\in e} S_f \widetilde{L_f} u_f$, and $\vec{u}_c = 1/2\,(V_c)^{-1} \sum_{f\in c} \left(S_f \widetilde{L_f} u_f\right)$, where $\widetilde{S_e}$ and $\widetilde{L_f}$ correspond with the wedge-dual surface and length of the primal edge and face, respectively. We will arrange them as

$$U_{stg} = \begin{pmatrix} U_e & \\ & U_c \end{pmatrix} \tag{7}$$

where $U_e$ and $U_c$ stand for the matrix arrangement of $\vec{u_e}$ and $\vec{u_c}$, as we did for $N$. Accordingly, $F = (\mathbb{I}_3 \otimes U)\,(\mathbb{I}_3 \otimes SP_{stg})\, N\phi_f$ produces a vector containing the fluxes of each $x$, $y$ and $z$ component of $\phi_f$ in $x$, $y$ and $z$ directions, i.e., a vector of 9 components for the edges and 9 components at the cells, so in total an 18 components vector!

The staggered divergence operator is then made up of the side and the base fluxes of the prism. These are considered in detail next.

**Side divergence.** Side faces are the result of the extrusion of each face edges. As such, their orientation is defined by $\hat{n_f} \times \hat{t_e}$, which is consistent with the orientation of the edge within the face. This can be seen in Figure 3.

Once the fluxes are defined, they are projected over the side normal and integrated over the side surface. Considering the flux of a single component, $\vec{F}^i$, we obtain $\vec{F_e}^{\,i} \cdot \left(\hat{n_f} \times \hat{t_e}\right) L_e \Delta x$.

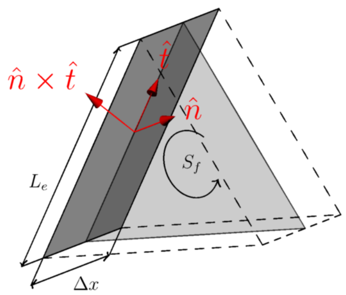


Figure 3: Reference coordinates for side faces.

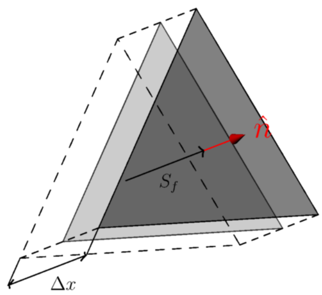


Figure 4: Reference coordinates for base faces.

In a finite volume setting, taking the divergence requires summing up all the contribution from the side fluxes and then dividing over the staggered volume as $(\Delta x S_f)^{-1} \sum_{e \in f} \pm \vec{F}_{ei} \cdot (\hat{n_f} \times \hat{t_e}) L_e \Delta x$. After rearranging, we obtain the side contributions as $\hat{n_f} \cdot S_f^{-1} \sum_{e \in f} \pm L_e \left( \hat{t_e} \times \vec{F_e}^i \right)$, from where we can recognize the curl operator $R$, which acts on every component of the flow. Note that the side contribution consists of the following three steps: taking the cross product with the tangential edge, taking the (oriented) sum over all edges and then taking the dot product with the face normal.

By introducing the following matrix

$$X(t) = \begin{pmatrix} 0 & -diag(t_z) & diag(t_y) \\ diag(t_z) & 0 & -diag(t_x) \\ -diag(t_y) & diag(t_x) & 0 \end{pmatrix} \tag{8}$$

we can represent the cross product $\hat{t_e} \times \vec{F_e}^i$ as the matrix operator $X(t)F_i$, where $F_i$ is the row vector $\vec{F_e}^i$. Finally, by introducing the projection over the normal by $N^T$ and using the Kronecker product to make $R$ act on all components, the contribution of the sides fluxes to the staggered control volume is $N^T (\mathbb{I}_3 \otimes R) X(t) F_e^i$.

**Base divergence.** Base fluxes are the product of the flow and the tensor at base faces (i.e., the ends). The base area is the same as the face in question, so its outer-oriented normal is readily defined by $\hat{n}_f$. Considering the flux of a single component, $\vec{F^i}$, the flow balance getting in or out of the face is determined by $\vec{F^i} \cdot \hat{n_f}$. Integrating over the surface and dividing over the staggered volume we get $(S_f \Delta x)^{-1} S_f \vec{F_i} \cdot \hat{n_f}$, which, after rearranging, we obtain the base contribution as $\hat{n_f} \cdot (\Delta x)^{-1} \sum_{c \in f} \pm \vec{F_c}^i$. From where we can recognize the gradient operator $\widetilde{G}$, which acts on each component of the flux. Gathering all components together we obtain, in matrix notation: $N^T \left( \mathbb{I}_3 \otimes \widetilde{G} \right) F_c^i$.

**Convective operator.** Now, adding both side and base contributions of the fluxes, we can obtain the staggered divergence as:

$$D_{stg} = N^T \left( \mathbb{I}_3 \otimes RX(t) \quad \mathbb{I}_3 \otimes \widetilde{G} \right) \tag{9}$$

Extending it for all $i$ gives the component-wise staggered convection $\mathbb{I}_3 \otimes (D_{stg} U_{stg} S P_{stg}) N$, as stated at the beginning of this section. In order to obtain the face-normal component of the vector variable, we need to project the resulting vector into the face normal again, yielding the final expression as:

$$C_{stg}(u) = N^T \mathbb{I}_3 \otimes (D_{stg} U_{stg} S P_{stg}) N \tag{10}$$

which has striking similarities with equation 4.

**Comparison with Cartesian mesh**

When applying this method method to a classical Cartesian mesh we recover the classical Harlow and Welch (1965) scheme. This can be seen as follows.

First, because of the orthogonal arrangement of the faces, we can distinguish between $x-$normal, $y-$normal and $z-$normal faces, i.e.: they only have contributions in one coordinate. Thus, the component-wise approach proposed here results in a fully decoupled set of equations. Second, face-to-cell and face-to-edge interpolation reduce to the classical symmetry-preserving $1/2$ scheme for the tensor variable. Third, because of the aforementioned orthogonal arrangement, the matrix $X(t)$ is also greatly simplified, such that only one row remain. This renders the classical side flows for the staggered control volume.

Finally, the interpolation of the fluxes is certainly imposed to collapse to the same discretization as the surface area–averaged detailed in Verstappen and Veldman (2003).

## 3 Preliminary results

As a preliminary stage, we assess the performance of other staggered discretizations constructed out of the collocated arrangement in the context of a classical channel flow at $Re_\tau = 180$. Details on the simulation can be found on Verstappen and Veldman (ibid.). In order to assess the impact of the convective scheme solely, we will restrict ourselves to the use of Cartesian meshes, so its eventual patologies are not imputable to mesh quality.

We compare the interpolation approach proposed in Zhang et al. (2002a) in Figure 5 with the standard symmetry-preserving staggered approach as in Verstappen and Veldman (2003) in Figure 6. While overall, results show convergence towards the reference solution, we make the following remarks:

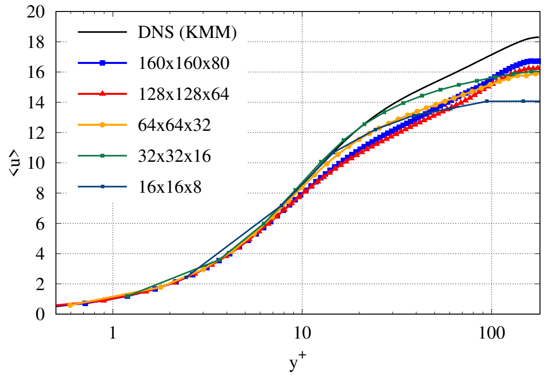


Figure 5: Mean velocity $\langle u \rangle$ profile of a channel flow at $Re_\tau = 180$. Computations are carried on a stretched Cartesian mesh. The staggered convective term is constructed by interpolation from cells to faces of the collocated convective term.

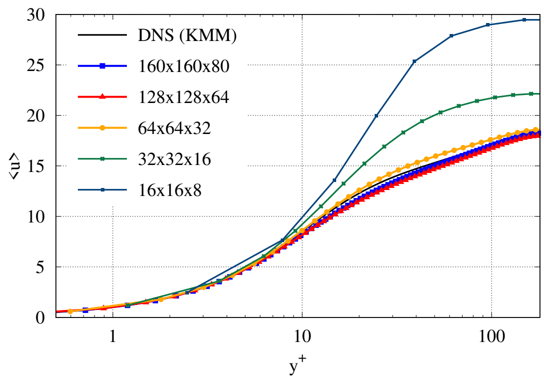


Figure 6: Mean velocity $\angle u \rangle$ profile for a channel flow at $Re_\tau = 180$. Computations are carried on a stretched Cartesian mesh. The staggered convective term is constructed with the present method, which collapses to the well-known approach of Harlow and Welch (1965).

First, for the interpolated approach, the linear regime is well captured until $y^+ \approx 10$ for all meshes, owing to the refinement near the wall, whereas the logarithmic region shows an erratic convergence: while coarse meshes, such as $32 \times 32 \times 16$ fit reasonably well up to $y^+ \approx 30$, finer meshes do no follow this trend but rather depart from the reference before, following a curve which ressembles the reference solution in slope, but slightly shifted downwards. On the contrary, the symmetry-preserving staggered approach shows a poorer performance for coarser meshes, while its convergence is consistent as the mesh is refined.

Second, convergence of the interpolated approach is sluggish and seems to stagnate below the expected centerline velocity. This is certainly in contrast the symmetry-preserving staggered formulation, which typically converge from an overpredicted centerline velocity towards the right value. While the reason of the later is the numerical diffusion included by the sub–resolution of the mesh, which laminarizes the flow, the reason for the underprediction of the centerline velocity is not clear for the construction of the interpolated scheme.

Beyond the purely observation of the unwanted convergence exhibit by staggered scheme constructed from direct approximation, we suggest a possible explanation in terms of the dispersion relation of the convective operator, as shown in Figure 7. While the staggered and collocated dispersion errors are well know, we observe a much more complex behavior of the interpolated schemes, which show a particular dispersion relation. This may suggest that the dispersion relation may be altering the turbulent spectra, introducing artificial turbulence which stop the flow beyond the expected physical mechanisms in the inertial regime. Interestingly though, the slope of the curve is well represented, while the ultimate reasons for the apparent shift downwards are, thus far, not self evident.

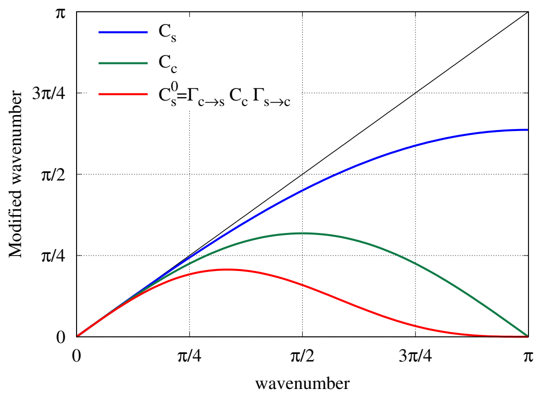


Figure 7: Dispersion relation for staggered (blue), collocated (green) and interpolated (red) convective operators.

## 4 Conclusions

A staggered formulation for unstructured meshes has been proposed in terms of elementary collocated operators. The resulting scheme collapses to the well-known staggered scheme proposed by Harlow and Welch (1965) when a Cartesian mesh is employed, as in Verstappen and Veldman (2003). This opens the door to he implementation of staggered formulation on readily available commercial codes.

By performing a dispersion relation analysis, we highlight that interpolation strategies for the construction of staggered methods from a collocated mesh substantially modify the dispersion relation, introducing undesired effects to the treatment of turbulence.

In future works, we plan to test this scheme in the context of unstructured meshes and, once the properties of the scheme have been cleared, assess its performance for the simulation of canonical turbulent flows.

## Acknowledgments

N.V.M and F.X.T. have been partially supported by the *Ministerio de Economía y Competitividad*, Spain, ANUMESOL project (ENE2017-88697-R).

## References

[1] Francis H. Harlow and J. Eddie Welch. "Numerical calculation of time-dependent viscous incompressible flow of fluid with free surface". In: *Phys. Fluids* 8.12 (1965), pp. 2182–2189.

[2] J. E. Hicken, F. E. Ham, J. Militzer, and M. Koksal. "A shift transformation for fully conservative methods: Turbulence simulation on complex, unstructured grids". In: *J. Comput. Phys.* 208.2 (2005), pp. 704–734.

[3] Kiyosi Horiuti and Takao Itami. "Truncation Error Analysis of the Rotational Form for the Convective Terms in the Navier-Stokes Equation". In: *J. Comput. Phys.* 145.2 (1998), pp. 671–692.

[4] Konstantin Lipnikov, Gianmarco Manzini, and Mikhail Shashkov. "Mimetic finite difference method". In: *J. Comput. Phys.* 257.PB (2014), pp. 1163–1227.

[5] Y. Morinishi, T. S. Lund, O. V. Vasilyev, and P. Moin. "Fully Conservative Higher Order Finite Difference Schemes for Incompressible Flow". In: *J. Comput. Phys.* 143.1 (1998), pp. 90–124.

[6] Blair Perot. "Conservation Properties of Unstructured Staggered Mesh Schemes". In: *J. Comput. Phys.* 159.1 (2000), pp. 58–89.

[7] C. M. Rhie and W. L. Chow. "Numerical study of the turbulent flow past an airfoil with trailing edge separation". In: *AIAA J.* 21.11 (1983), pp. 1525–1532.

[8] Enzo Tonti. *On the formal structure of physical theories*. 1975.

[9] Enzo Tonti. "Why starting from differential equations for computational physics?" In: *J. Comput. Phys.* 257.PB (Jan. 2014), pp. 1260–1290.

[10] F. X. Trias, O. Lehmkuhl, A. Oliva, C. D. Pérez-Segarra, and R. W. C. P. Verstappen. "Symmetry-preserving discretization of Navier–Stokes equations on collocated unstructured grids". In: *J. Comput. Phys.* 258 (Feb. 2014), pp. 246–267.

[11] F. X. Trias, N. Valle, A. Gorobets, and A. Oliva. "Symmetry-Preserving Discretization of Navier-Stokes On Unstructured Grids: Collocated Vs Staggered". In: *ECCOMAS Congr. 2020*. January. 2021, pp. 11–15.

[12] Evan VanderZee, Anil N. Hirani, Damrong Guoy, and Edgar A. Ramos. "Well-Centered Triangulation". In: *SIAM J. Sci. Comput.* 31.6 (Jan. 2010), pp. 4497–4523.

[13] Oleg V. Vasilyev. "High Order Finite Difference Schemes on Non-uniform Meshes with Good Conservation Properties". In: *J. Comput. Phys.* 157.2 (2000), pp. 746–761.

[14] R. W. C. P. Verstappen and A. E. P. Veldman. "Direct numerical simulation of turbulence at lower costs". In: *J. Eng. Math.* c (1997), pp. 143–159.

[15] R. W. C. P. Verstappen and A. E. P. Veldman. "Symmetry-preserving discretization of turbulent flow". In: *J. Comput. Phys.* 187.1 (2003), pp. 343–368.

[16] Xing Zhang, David Schmidt, and Blair Perot. "Accuracy and conservation properties of a three-dimensional unstructured staggered mesh scheme for fluid dynamics". In: *J. Comput. Phys.* 175.2 (2002), pp. 764–791.

[17] Xing Zhang, David Schmidt, and J. Blair Perot. "Accuracy and Conservation Properties of a Three-Dimensional Unstructured Staggered Mesh Scheme for Fluid Dynamics". In: *J. Comput. Phys.* 175.2 (2002), pp. 764–791.